AIAA JOURNAL
Vol. 48, No. 5, May 2010

Technical Notes

Penetration Characteristics of Film-Cooling Jets at High Blowing Ratio

Lamyaa El-Gabry
American University in Cairo, New Cairo, 11835 Arab Republic of Egypt
James Heidmann
NASA John H. Glenn Research Center at Lewis Field, Cleveland, Ohio 44135
and
Ali Ameri
Ohio State University, Columbus, Ohio 43210

DOI: 10.2514/1.42611

Introduction

FILM cooling is one of the most heavily used cooling methods in gas turbines. Film-cooling holes are machined through the surface of turbine airfoils, and coolant air is bled from cavities within the airfoil, through the film holes, to form a protective layer between the airfoil external surface and the hot gas. At high blowing ratios, the coolant can jet or blow off, allowing the hot gas to cover the surface, resulting in reduced effectiveness. There are many design options presented in the open literature that attempt to reduce the jetting effect at the high blowing ratio. Bunker [1] reviews more than 30 years worth of literature on shaped film cooling alone. In shaped film holes, the cross section of the hole expands at the exit to the freestream, thereby decreasing the velocity of the jet and lowering its trajectory, enabling it to lay closer to the surface.

Detailed descriptions of the flow structures within the film-cooling hole, obtained experimentally and numerically [2], show several vortex structures, including the counter-rotating kidney pair of vortices. This vortex pair is responsible for the downwash of hot gas from the freestream down toward the wall, thereby reducing the effectiveness. In an attempt to counter those vortices, a concept was developed at NASA John H. Glenn Research Center [3] that includes the use of cylindrical side holes that are fed from the main film-cooling hole. There are also concepts put forth to increase film effectiveness by adjusting the conditions outside of the hole, such as a ramp upstream of the hole [4] or a geometric obstacle downstream [5] to increase mixing between the coolant and the freestream.

Whatever means are used to increase effectiveness, be it through changes in the coolant-hole geometry or changes in the upstream or downstream conditions, it is often desirable to evaluate these concepts numerically before embarking on experimental validation. Therefore, it is important for the gas-turbine heat-transfer design community to be able to have design tools capable of predicting performance or film effectiveness for simple as well as complex geometries. There are many numerical studies of film cooling; too numerous to list here. The bibliography alone of film-cooling computational fluid dynamics (CFD) works through 1996, compiled by Kercher [6], is in excess of 10 pages, and from 1996 through the present, there are at least that many (if not more) published works on film-cooling CFD. There remains a significant challenge, and that is at high blowing ratios. Reynolds-Averaged Navier–Stokes (RANS)-based CFD models underpredict film effectiveness severely; in some regions, by up to a factor of four [3]. Although large-eddy simulation (LES) has shown promise in capturing wake vortex structures and mixing, these methods have a long turnaround time, making them unsuitable for typical design cycles. The objective of this study is to use RANS-based CFD methods to analyze film cooling at high blowing ratios and compare numerical predictions with experimental data to identify shortcomings of these models in predicting film-cooling flows.

Received 6 December 2008; revision received 14 February 2010; accepted for publication 16 February 2010.

Experimental Data for Comparison

Table 1 shows the plenum pressure, outlet pressure, and plenum temperature for each test condition analyzed. The ratios refer to jet to mainstream (i.e., density ratio $= \rho_j/\rho_\infty$, blowing ratio$= \rho_j U_j/\rho_\infty U_\infty$, and velocity ratio $= U_j/U_\infty$).

Case 1 is a 30-deg cylindrical film hole with a density ratio, a blowing ratio, and a velocity ratio of roughly one. The plenum pressure and temperature and the back pressure were adjusted to match the density ratio, blowing ratio, and velocity ratio. The test results include local and span-averaged film effectiveness. Details on this case can be found in [7].

For cases 2 through 4, the test data of Thole et al. [8] and Sinha et al. [9] will be used for comparison with CFD results. Thole et al. [8] measured air temperatures along the jet centerline for round film holes inclined at 35 deg along the flow direction, with spacing of three-hole diameters ($X/D = 3$) with a length of $L/D = 3$. There were nine cases reported; the case having the highest blowing ratio was selected for comparison. Case 2 is the highest blowing-ratio case reported [8] and was chosen because it represents a worst-case scenario in which the film is most likely to jet or lift from the surface. The test data available for case 2 include fluid temperatures along the centerline of the jet; there is no film-effectiveness data available for this high-blowing-ratio case.

Sinha et al. [9] used the same test facility at the University of Texas at Austin as Thole et al. [8] but made different measurements. Sinha et al. [9] measured film effectiveness. Case 3 is a film-cooling hole at a low blowing ratio of 0.5, a density ratio of 2, and a velocity ratio of 0.25. The pressure boundary conditions used to match the test data are shown in Table 1. The centerline air temperatures for case 3 are found in [8], and the centerline and span-averaged film effectiveness were measured by Sinha et al. [9]. Case 4 is at an intermediate blowing ratio of 0.78 and was selected because it represents the highest blowing ratio for which there is both fluid temperature data in [8] and film effectiveness data in [9].

Computational Method

The computational domain extends from the freestream inlet, located 19 hole diameters upstream of the film-cooling-hole leading edge to be consistent with the experiment. The outlet is located 30 hole diameters downstream. Symmetry boundary conditions are applied along the jet centerline and along the line of symmetry between two adjacent jets. The plenum extents in the streamwise direction are chosen to match the experimental test setup. The height of the freestream channel is 10 hole diameters, for which an inviscid-slip boundary condition is applied.

A multiblock structured grid was used for this domain. Near-wall grid clustering is used to enable modeling of the viscous sublayer, using wall integration techniques. The first cell height is $1E-3$ hole

Table 1 Test cases and corresponding inlet and outlet conditions

Case	Density ratio	Blowing ratio	Velocity ratio	Plenum pressure	Plenum temp.	Back pressure	Reference
1	1.05	1	0.95	1.0392	0.95	0.97	Dunghel et al. [7]
2	2	2	1	1.16	0.53	0.94	Thole et al. [8]
3	2	0.5	0.25	0.96	0.53	0.94	Thole et al. [8]Sinha et al.[9]
4	1.2	0.78	0.65	0.999	0.82	0.933	Thole et al. [8]Sinha et al.[9]

diameters, which yields a dimensionless $Y+$ of one or less at all walls. The stretching ratio is less than 1.2. There are 56 nodes across the film-cooling hole, and 40 nodes are in the spanwise direction (which is half a pitch). The grid has a total of $\sim$1.5 million cells and 1.7 million nodes. Grid independence was verified in a prior study [7] for one of the cases, and the same grid topology was then used for all grids generated for this study. Figure 1 shows the extents of the domain and the grid, and Fig. 2 is a close up of the grid near the film hole exit.

The CFD code used in this study is Glenn-HT, an in-house research code developed at the NASA John H. Glenn Research Center. Details on the Glenn-HT code are in [10]. The code solves the RANS equations for compressible flow using finite-volume discretization that is second-order accurate in time and space. It uses the low Reynolds-number k–ω model of Wilcox [11], which integrates to the wall; therefore, no wall functions are used to model the viscous sublayer.

Results and Discussion

High-Blowing-Ratio Case Comparison

The CFD underpredicts the film effectiveness considerably for case 1 (also shown in [7]). Case 2 is also at high blowing; however, there is no film effectiveness reported in the test measurements. Figure 3a shows the experimental results for centerline temperatures, and Fig. 3b shows the CFD results.

In the contour plots shown, X is the streamwise distance and Y is the normal distance from the wall. Dimensionless temperature is given by $\theta = (T - T_\infty)/(T_c - T_\infty)$; by definition, contours of 1.0 indicate coolant temperature and contours of 0.0 indicate freestream temperature. Comparing Fig. 3b with the experimental results of Fig. 3a, one sees that the CFD was able to capture the vertical extent of the mixing accurately; the CFD shows that the mixing region extends two hole diameters from the wall, as did the experimental results. However, there is discrepancy in the near-wall region downstream of the cooling hole; CFD results show high temperatures in this region (θ of 0.1 and below), whereas the experimental results show cooler temperatures (θ of 0.3 to 0.4).

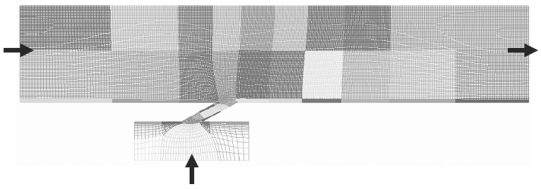

Fig. 1 Computational domain showing block structured grid.

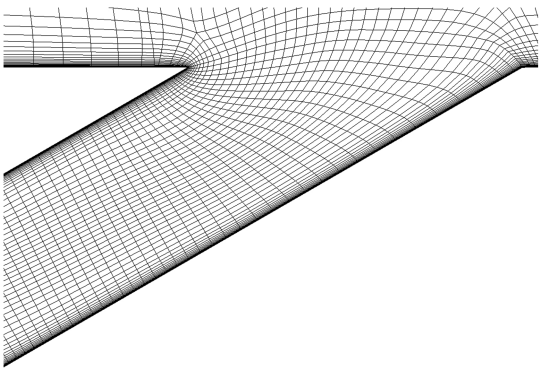

Fig. 2 Close up of viscous grid near the hole exit.

Low-Blowing-Ratio Case Comparison

The next case to be considered is case 3 in Table 1. This case is chosen because, in addition to the measurements of the temperature field along the jet centerline, there are also measurements of film effectiveness. Figure 4a shows the experimental dimensionless

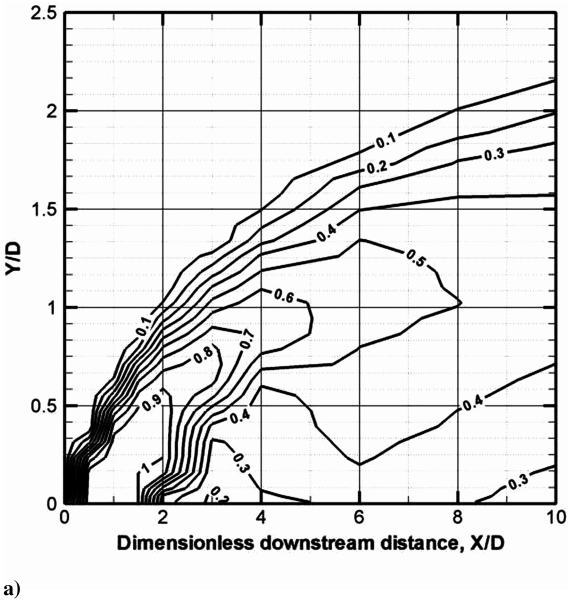

a)

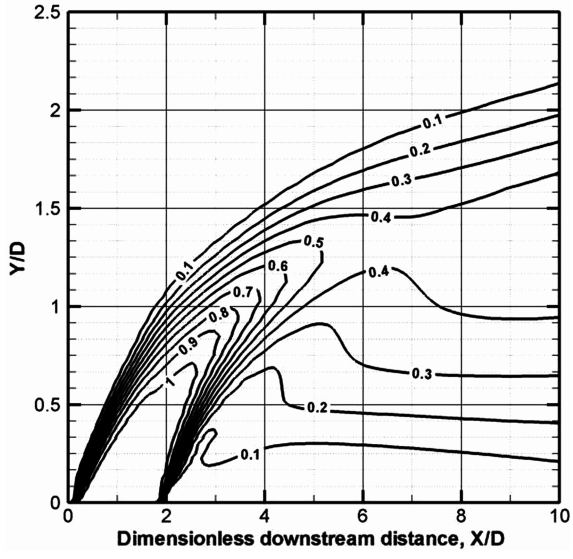

b)

Fig. 3 Case 2: a) experimental [8] and b) numerical predictions of dimensionless temperature contours along jet centerline.

temperature contours along the jet centerline for case 3, and Fig. 4b shows the CFD predictions.

The CFD predicts near-wall temperatures in the range of 0.9 to 0.4, which is in line with the measurements in Fig. 4a. The lateral extent of the film is accurately predicted by the CFD model, which shows the film extending to one hole diameter from the wall. However, there is a difference in the contour lines near the wall. The lines of the experiment suggest smaller gradients in temperature near the wall (the lines are more vertical), whereas the CFD shows contour lines that are more angled and indicative of larger temperature gradients in the wall-normal direction.

Figure 4c shows the comparison between the measured and CFD-predicted centerline film effectiveness, which is defined as the ratio of difference between the freestream and adiabatic wall temperature to the difference between the freestream and coolant temperature (i.e., $=(T_\infty - T_{aw})/(T_\infty - T_c)$). The agreement between the measured and CFD-predicted centerline film effectiveness is good, which is consistent with the good agreement between the measured and predicted temperature contours along the jet centerline in Figs. 4a and 4b.

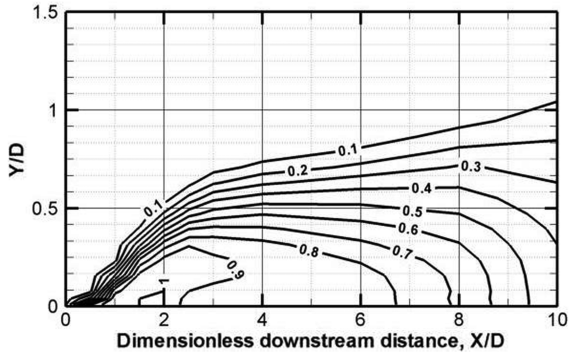

a)

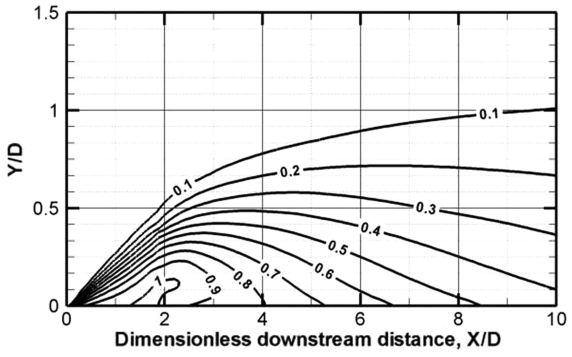

b)

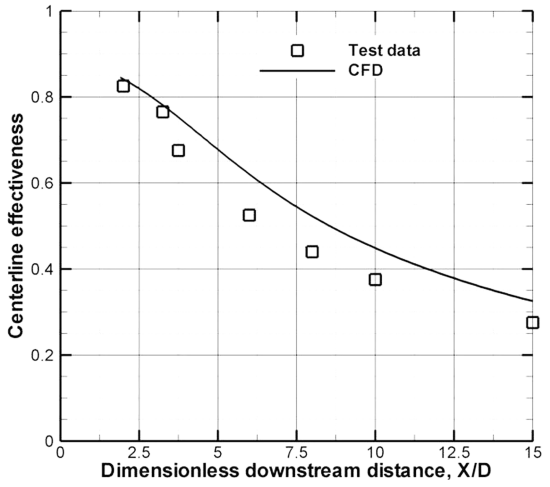

c)

Fig. 4 Case 3: a) experimental [8], b) numerical prediction of dimensionless temperature contours along jet centerline, and c) comparison of measured and predicted centerline film effectiveness [9].

Intermediate-Blowing-Ratio Case Comparison

Up to this point, results have been presented for a high-blowing-ratio case in which the film is detached from the surface and a low-blowing-ratio case in which the film remains attached to the surface. Case 4 offers an intermediate blowing ratio. CFD predictions of the temperature contours at the jet centerline are compared with data from Thole et al. [8], and film effectiveness at the centerline is compared with measurements of Sinha et al. [9].

Figure 5a shows the measured fluid temperatures along the jet centerline [8], and Fig. 5b shows the CFD predictions for the same case. Figure 5b suggests that the CFD is overpredicting the extent of the film-effected region from the wall. It also shows larger gradients of temperature in the wall-normal direction, which was also evident in Figs. 4a and 4b, but it is now even more pronounced at this higher blowing ratio. There is fair agreement in the magnitude of the fluid temperatures in the near-wall region in the wake of the jet; the test results in Fig. 5a show near-wall temperatures ranging from 0.6 to 0.4, and the CFD predicts temperatures ranging from 0.5 to 0.6 in this same region.

The CFD prediction of centerline film effectiveness is shown in Fig. 5c, along with experimental measurements. The CFD predicts a constant decrease in effectiveness along the streamwise direction, with little variation as compared with the test measurements that show higher variability. This is, perhaps, a consequence of the difference in the contour line pattern, whereas the CFD contour lines in Fig. 5b are nearly horizontal with the flow (meaning a fairly uniform near-wall temperature distribution), the test results show contours that are not horizontal, suggesting greater mixing in the wall-normal direction in the wake region.

Figure 5d shows the comparison between the measured span-averaged film effectiveness [9] and the CFD-predicted effectiveness, which are in excellent agreement despite the differences in the centerline temperature contours. This could be due to the good agreement in the magnitude of near-wall temperature predictions and the fact that spanwise averaging washes out differences in local effects.

Conclusions

A series of CFD models were developed to simulate flat-plate film cooling, with particular interest in high-blowing-ratio cases in which the film is detached from the surface. Four data sets were used in evaluating the CFD predictions, which collectively include measurements of fluid temperatures along the centerline and some measurements of centerline and spanwise-averaged film effectiveness.

For high-blowing-ratio cases, the CFD underpredicts the mixing in the wake region of the jet. The CFD is able to predict the vertical extent of the film-effected region, but it underpredicts the vertical mixing in the wake of the jet, which results in underpredicting the film effectiveness for high-blowing-ratio detached films.

For the low-blowing-ratio case, the flow is not separated; therefore, the predictions of fluid temperatures along the centerline agree well with test measurements. Consequently, the CFD-predicted film effectiveness along the jet centerline is also in good agreement with test data.

At the low and intermediate blowing ratio, the CFD contours of fluid temperatures along the centerline are nearly horizontal with the flow, meaning a fairly uniform near-wall temperature, whereas the test results show contours that are not horizontal, suggesting greater mixing in the wall-normal direction in the wake region. At the intermediate blowing ratio, this difference is more pronounced than at the lower blowing ratio and results in overprediction of the centerline film effectiveness. Nevertheless, on a spanwise-averaged basis, at the intermediate blowing ratio, the CFD predictions of film

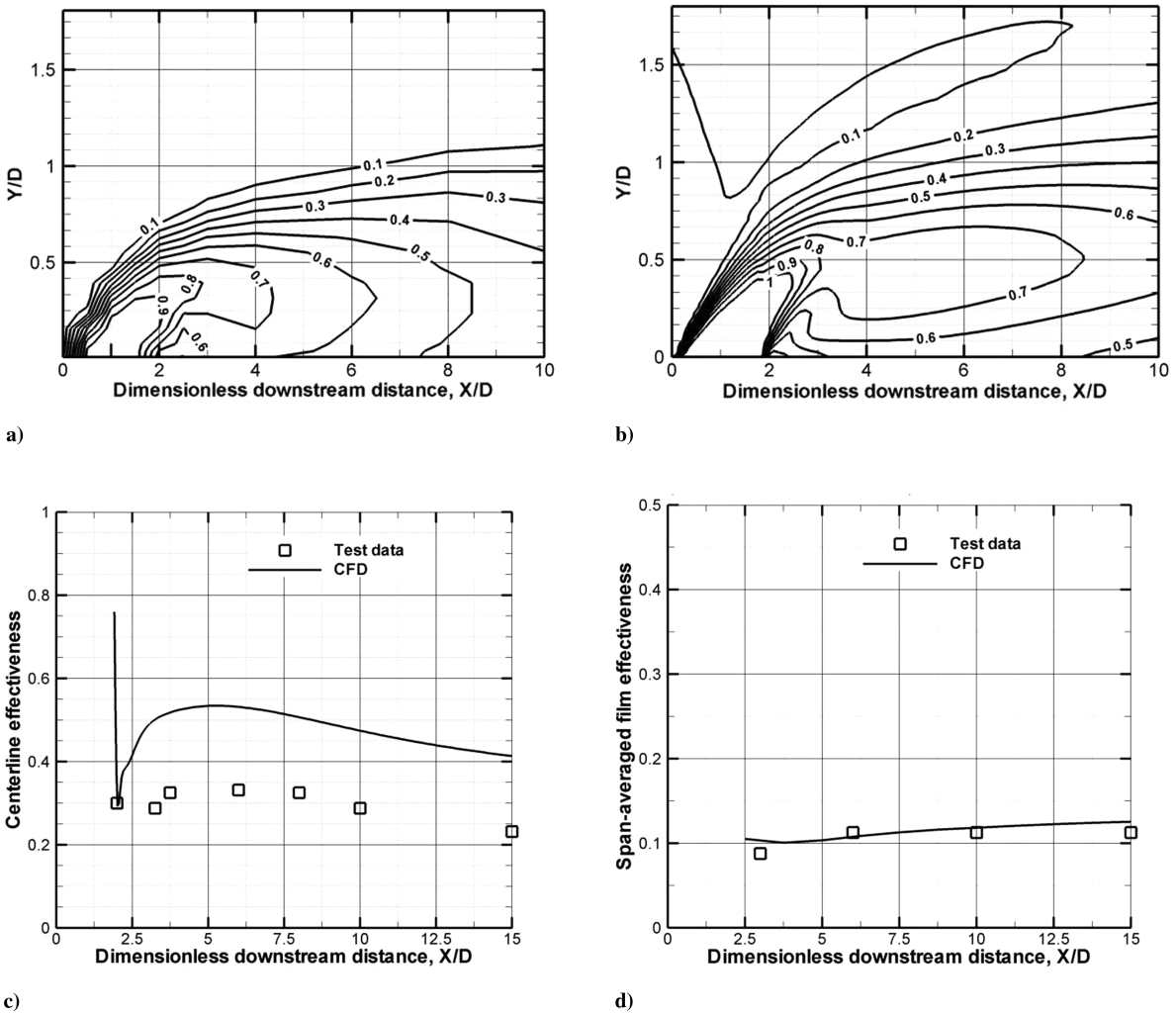

Fig. 5 Case 4: a) experimental [8], b) numerical prediction of dimensionless temperature contours along jet centerline, c) comparison of measured and predicted centerline film effectiveness [9], and d) comparison of measured and predicted span-averaged film effectiveness [9].

effectiveness are in good agreement with test measurements, despite the overprediction at the centerline.

Overall, the results of this study suggest that the wake of the jet represents an area of challenge for the RANS-based CFD models evaluated, more so at high blowing ratios in which the jet is separated. The highly unsteady nature of separated flows is difficult to capture with steady or maybe even unsteady RANS (URANS) models, which could also average out the unsteady features as a result of the ensemble averaging or Reynolds averaging. Turbulence models are formulated to model the Reynolds stress terms, which are in themselves averages of fluctuations, and so it is possible that, even with URANS methods, the turbulence models could still be ineffective. Despite the shortcomings, RANS methods remain important, as they are more practical than LES, for instance, in terms of use in design. Therefore, efforts to address the modeling/validation gap between experiment and CFD results should continue. This will require additional field data; particularly, measurements of the flowfield in the wake of the film, including not only temperatures but also velocity and turbulence fluctuations along spanwise and streamwise planes to fully characterize the mixing and identify the specific root cause of the validation gap (for example, anisotropy, unsteadiness, or other factors).

Acknowledgments

The authors would like to acknowledge the cooperation of David Bogard of the University of Texas at Austin for providing the test data used in the comparisons throughout this paper. The first author would also like to thank the NASA Glenn Faculty Fellowship Program for support of this research.

References

[1] Bunker, R. S., "A Review of Shaped Hole Turbine Cooling Technology," *Journal of Heat Transfer*, Vol. 127, No. 4, 2005, pp. 441–453.
doi:10.1115/1.1860562

[2] Leboeuf, F. and Sgarzi, O, "The Detailed Structure and Behavior of Discrete Cooling Jets in a Turbine," *Annals of the New York Academy of Sciences*, Heat Transfer in Gas Turbine Systems, Vol. 934, Heat Transfer in Gas Turbine Systems, May 2001, pp. 95–109.

[3] Heidmann, J., and Ekkad, S. V., "A Novel Antivortex Turbine Film-Cooling Hole Concept," *Journal of Turbomachinery*, Vol. 130, No. 3, July 2008, Paper 03120.
doi:10.1115/1.2777194

[4] Na, S., and T. Shih, "Increasing Adiabatic Film-Cooling Effectiveness by Using an Upstream Ramp," *Journal of Heat Transfer*, Vol. 129, No. 4, 2007, pp. 464–471.
doi:10.1115/1.2709965

[5] Rigby, D. L., and Heidmann, J., "Improved Film Cooling Effectiveness by Placing a Vortex Generator Downstream of Each Hole," IGTI and ASME Turbo Expo, American Society of Mechanical Engineers Paper GT2008-51361, New York, 2008.

[6] Kercher, D. M., "A Film-Cooling CFD Bibliography: 1971–1996," *International Journal of Rotating Machinery*, Vol. 4, No. 1, 1998, pp. 61–72.
doi:10.1155/S1023621X98000062

[7] Dhungel, S., Phillips, A., Ekkad, S. V., and Heidmann, J. D., "Experimental Investigation of a Novel Anti-Vortex Film Cooling Hole

Design," IGTI and ASME Turbo Expo, American Society of Mechanical Engineers Paper GT2007-27419, New York, 2007.

[8] Thole, K. A., Sinha, A. K., Bogard, D. G., and Crawford, M. E., "Mean Temperature Measurements of Jets with a Crossflow for Gas Turbine Film Cooling Applications," *Rotating Machinery: Transport Phenomena, Proceedings of the 3rd International Symposium on Transport Phenomena and Dynamics of Rotating Machinery*, Taylor and Francis, Washington, D.C., 1990, pp. 69–85.

[9] Sinha, A. K., Bogard, D. G., and Crawford, M. E., "Film-Cooling Effectiveness Downtream of a Single Row of Holes with Variable Density Ratio," *Journal of Turbomachinery*, Vol. 113, No. 3, 1991, pp. 442–449.
doi:10.1115/1.2927894

[10] Steinthorsson, E., Liou, M.-S., and Povinelli, L. A., "Development of an Explicit Multiblock/Multigrid Flow Solver for Viscous Flows in Complex Geometries," AIAA Paper No. 93-2380, 1993.

[11] Wilcox, D. C., "Simulation of Transition with a Two-Equation Turbulence Model," *AIAA Journal*, Vol. 32, No. 2, 1994, pp. 247–255.
doi:10.2514/3.59994

J. Sahu
Associate Editor